Available online at www.sciencedirect.com
ScienceDirect
Energy Reports 8 (2022) 1381–1393
www.elsevier.com/locate/egyr

TMREES22-Fr, EURACA, 09 to 11 May 2022, Metz-Grand Est, France

Design and off-design system simulation of concentrated solar super-critical CO2 cycle integrating a radial turbine meanline model

Michael Deligant[a,*], Moritz Huebel[b], Tchable-Nan Djaname[a], Florent Ravelet[a], Mathieu Specklin[a], Mohamed Kebdani[a]

[a] *Arts et Metiers Institute of Technology, CNAM, LIFSE, HESAM University, Paris, France*
[b] *Modelon, Baumwall 7, 20459 Hamburg, Germany*

Received 7 July 2022; accepted 21 July 2022
Available online xxxx

Abstract

The proper design of a Concentrated solar power (CSP) plant and the associated thermal energy storage requires a careful analysis of the yearly expected irradiance and environmental conditions. System simulations based on accurate components models allow the prediction of the performance of the plant and the analysis of the components interactions. The simulations of various scenarios provide information that will help tuning the design of the components to improve the performance of the whole system at design and off-design conditions. In this paper, the focus is set on the radial turbine expander which is one of the most important component. Classical system simulation approaches use map based performance model for the turbine. This require to generate the performance map either with meanline models, CFD simulations or experiments. This is not very convenient when iterating on the system design and if the actual turbine does not exist yet. In this work, a meanline model for radial inflow turbine operating with real gas has been implemented in MODELICA language for the first time to the authors' best knowledge. This turbine model has been coupled with the available CSP sCO2 Brayton cycle model in MODELON ThermalPower library. A parametric study on a virtual test bench show the turbine performances for various rotational speed and inlet guide vane angle. The study focus then on the performance prediction of on and off design of the system with a 8 MW turbine obtained with a simple preliminary design calculation. The investigations showed that for the varying load conditions in the solar plant system, an improved operating point has been identified by adjusting the rotational speed and the inlet guide vane angle. Future work will focus on the use such system model with multi objective meta heuristic optimization.

Peer-review under responsibility of the scientific committee of the TMREES22-Fr, EURACA, 2022.

Keywords: System modeling; Radial turbine; CO2; Concentrated solar; Meanline

1. Introduction

Concentrated solar is one the renewable energy solutions to reduce the carbon footprint of electricity production. Power plants with organic Rankine cycle (ORC) or Brayton cycle with super critical CO2 (sCO2) are the two most

* Corresponding author.
E-mail addresses: michael.deligant@ensam.eu (M. Deligant), moritz.hubel@modelon.com (M. Huebel).

https://doi.org/10.1016/j.egyr.2022.07.141

Peer-review under responsibility of the scientific committee of the TMREES22-Fr, EURACA, 2022.

promising thermodynamic cycles [1,2]. However, varying environmental conditions and solar irradiance can affect the electricity output of such systems and need to be carefully simulated for the proper design of a CSP plant and the associated thermal energy storage [3,4]. The performances of energy conversion systems from thermal to electricity rely on the appropriate sizing and design of interacting components [5,6]. A lot of effort has been made with the development of the open-source libraries by Casella with ThermoPower [7] and Quoilin with Thermocycle [8]. When designing a complex system for a given set of steady or fluctuating operating conditions, very simple models are often used to predict the performance of each component. For example, the efficiency of the turbine or the pinch of the heat exchangers are assumed to be constant [9]. The design process is thus run with iterative loops until convergence of the design parameters that give the expected results. The detailed design of the components themselves are then optimized to fit the required design parameters.

Turbomachines have usually an important place in energy conversions systems. In ORC and sCO2 systems it is probably the most important component to be optimized for design and off-design operation [10,11]. Indeed, a small improvement of the turbine efficiency can greatly contribute to the economic profitability of the system by directly increasing the electricity output without changing the other components.

For turbines in power plants specifically, dynamic system simulation covers a wide range of applications resulting in economic, safety and efficiency improvements both for operation and design. Most conventional “onDesign” approaches take only one nominal operating point into account to size components for a system for the optimal efficiency. Sielemann et al. [12] showed for turbine design, how considering multiple operation points already improves the system efficiency for the actual operation significantly. Also for a fixed system design, transient behavior often is investigated using dynamic models. Most energy systems show relevant behavior that cannot be captured with a collection of steady-state points at all. Wittenburg [13] shows how storing and releasing thermal energy in a transient process leads to exergetic losses affecting efficiency. Also, thermal and mechanical component stress which is often limiting load gradients and therefore affecting plant behavior can easily be captured using dynamic power plant models [14]. The most commonly used application for dynamics system models however is to improve the interaction of dynamic processes and controls, e.g. for startup [15], providing ancillary services [16] and failure mode [17] scenarios. The economic relevance of optimizing dynamic operation is shown in [18].

In this paper, a meanline model predicting the full performance of any radial turbine is implemented in MODELICA language inside MODELON IMPACT platform and coupled with MODELON libraries VaporCycle and ThermalPower. VaporCycle provides thermodynamic properties of any fluids, organic Rankine cycles and vapor compression cycles (Brayton) components and systems models. Thermal power provides models for solar collectors, thermal energy storage and replaceable power cycle models (Rankine, Brayton, ORC).This allow the use of the developed turbine model inside existing ORC cycle and solar super critical CO2 cycle using two-phase media equations for CO2 including real gas correlations for the super-critical region [19,20]. In comparison to steady-state tools, this transient implementation also allows to consider design-critical constraints such as thermal and mechanical stress of critical components as well as control design. Specifically for sCO2 power cycles, operating with compressor inlet conditions near the critical point, a stable operating point is hard to achieve in practice as measurable temperature and pressure near the critical point are almost constant and depending fluid properties such as heat capacity changes significantly and in a very non-linear way. A dynamic investigation tool is therefore mandatory prerequisite to find an efficient system design in practice. The novelty of the proposed approach is the possibility to get turbine performance prediction at early design stage directly from geometrical parameters that can also be tuned to optimized the system global performances.

2. Radial turbine

The radial turbine is composed of scroll housing, a vanned distributor, a rotor and an exit pipe. The definition of the geometrical parameters and stations numbers are presented in Fig. 1.

2.1. Equations

The meanline analysis consists in the prediction of the turbine performance given its geometry and operating conditions. This type of computation relies on the analysis of the velocity triangle, based on main geometrical parameters (see Fig. 2) and loss models describing the principle mechanisms for energy degradation inside the turbine. Although meanline methods cannot provide a detailed analysis of the flow structures inside a machine,

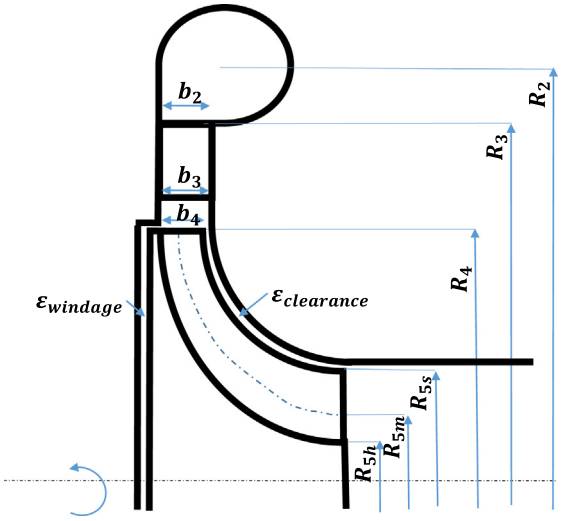

Fig. 1. Schematic view of the turbine with geometric parameters.

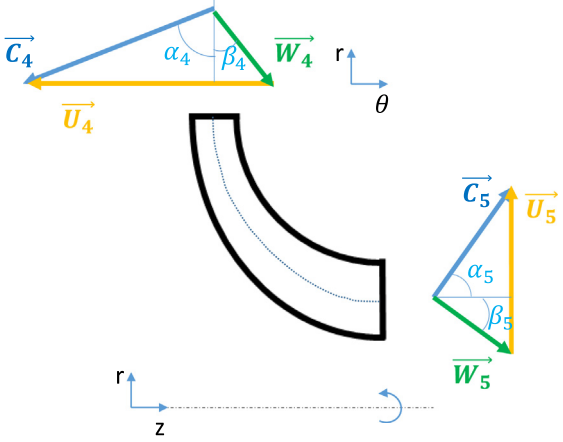

Fig. 2. Rotor inlet and outet velocity triangles.

the proposed models are generally validated using numerical simulations and experimental data [21]. Hence, after validation, they become a useful instrument for optimizing the radial inflow turbine performance.

In this study, the models used for the meanline analysis are adapted from the best combination proposed by Persky and Sauret in [21] for ORC and sCO2 radial turbines among the loss models available in the literature. As refrigerant and sCO2 do not behave like ideal gas, all fluid properties are determined via the thermodynamic library CoolProp [22], which depicts real gas behavior.

The expander efficiency can be expressed as Eq. (1)

$$\eta_{ts} = \frac{\Delta h_0}{\Delta h_0 + \Delta h_{losses}} - \Delta\eta_{cl} \tag{1}$$

where Δh_0 is the real total to static enthalpy variation through the turbine and Δh_{losses} is the summation of the different losses (incidence, trailing edge, passage, exit, windage) and $\Delta\eta_{cl}$ it the efficiency reduction due the clearance losses.

The total enthalpy is computed from the static enthalpy Eq. (2) and the fluid velocity C. The velocity is computed from the area and the density ρ using CoolProp library [20] with static conditions.

$$h_0 = h + \frac{1}{2}C^2 \tag{2}$$

The scroll housing and the vanned distributor guide and accelerate the fluid from stagnation inlet condition with nearly null velocity ($C_0 = 0$) up to the rotor inlet condition C_4 with the absolute flow angle d α_4. Assuming conservation of total enthalpy and ideal isentropic acceleration of the fluid from 0 to 4, the conditions in station 4 can be computed from the following Eqs. (3) to (7):

$$h_{04} = h_{00} = h_4 + \frac{1}{2}C_4^2 \tag{3}$$

$$\rho_4 = PropsSI(P_4, h_4) \tag{4}$$

$$C_{4r} = \frac{\dot{m}_{CO_2}/\rho_4}{2\pi R_4 b_4} \tag{5}$$

$$P_4 = PropsSI(h_4, s_0) \tag{6}$$

$$\tan(\alpha_4) = \frac{C_{4r}}{C_{\theta 4}} \tag{7}$$

The loss models used in this study are summarized here below:

- Incidence losses, from Wasserbauer and Glassman [23]:

$$\Delta h_i = \frac{1}{2}W_{in}^2 \sin^2(\beta_{in} - \beta_{in,opt}) \tag{8}$$

with $\beta_{in,opt} = \tan^{-1}[\frac{-1.98\tan(\alpha_{in})}{Z_r(1-\frac{-1.98}{Z_r})}]$;

- Passage losses from Wasserbauer and Glassman [23]:

$$\Delta h_p = \frac{1}{2}K[W_{in}^2 \cos^2(\beta_{in} - \beta_{in,opt}) + W_{out}^2] \tag{9}$$

where K is a coefficient which must be determined by comparison with experiments.

- Trailing edge losses from Qi et al. [24]:

$$\Delta h_{te} = \frac{\Delta P_{0,out,rel}}{\rho_{out}} \tag{10}$$

where $\Delta P_{0,out,rel} = \frac{\rho_5 w_5^2}{2g_c}[\frac{Z_r + t_r}{\pi(R_{5s}+R_{5h})\cos(\beta_{5,rms})}]$
and g_c is the force–mass conversion constant equal to one when using SI units;

- Exit losses from Erbas et al. [25]:

$$\Delta h_e = (1 - C_d)\frac{C_{out}^2}{2} \tag{11}$$

where $C_d = -3.25 \cdot 10^{-4}|\alpha_{exit}|^2 + 6.25 \cdot 10^{-3}|\alpha_{exit}| + 0.57$;

- Windage losses from Qi et al. [24]:

$$\Delta h_w = \frac{\rho_4 U_4^3 R_4^2 Cm}{2\dot{m}} \tag{12}$$

where the model coefficient C_m is based on the experiments by Daily and Nece [26] and computed as follows:

$$C_m = \frac{C\left(\frac{eb}{R_4}\right)^m}{Re^n} \tag{13}$$

being C, m and n dependent on the turbulence regime [27] as determined by Re_r:

$$Re_r = \frac{\rho_4 \omega R_4^2}{\mu_4} \tag{14}$$

Table 1. Turbine geometrical parameters.

Parameters	Values	Units
Inlet radius R_4	122.60	mm
Inlet tip b_4	12.31	mm
Relative inlet angle β_4	90	°
Absolute inlet angle α_4	76	°
Outlet radius at hub R_{5h}	36.78	mm
Outlet radius at shroud R_{5s}	73.67	mm
Rotor height Z	55.34	mm
Relative outlet angle at hub β_{5h}	60.35	°
Relative outlet angle at shroud β_{5s}	41.26	°
Number of blades Z_r	15	–

- Clearance losses from Rodgers [28]:

$$\Delta\eta_{cl} = 2\frac{\varepsilon_{clearance}}{R_4}\left(\frac{R_{5s}}{R_4} - 0.275\right) \tag{15}$$

3. Concentrated solar power

3.1. Solar plant

The reference system for the following investigation is a central receiver concentrated solar power system, based on a model of the 12.5 MW (rated gross electrical output) Solar Two test facility in California, USA [29]. The plant model contains the following components:

- Central receiver components including an insolation model, heliostats, a receiver and storage tanks. Solar salt is used as heat transfer and heat storage medium.
- Electrical power generator system as been adapted to work with a recompression Brayton cycle using supercritical carbon dioxide. The Brayton cycle consists of two compressors, turbine, high temperature and low temperature recupertors, cooler and primary heater where Molten salt will provide heat to the Brayton cycle working fluid [30].
- Control system containing a number of PI controllers, determining pump speeds to provide sufficient heat to the Brayton cycle fluid.

The plant model is based on the Modelica language and is accessible in Modelon's ThermalPower Library. Fig. 3 shows the top level schematic and the operating conditions for an intermediate load point within the modeling and simulation platform Modelon Impact.

3.2. sCO2 turbine characteristics

For the CSP plant, the turbine (Fig. 4) was designed with the preliminary calculations presented by Aungier in [31]. The design parameters are $P_{inlet} = 205$ bar, $P_{outlet} = 86$ bar, $\dot{m} = 84\ \mathrm{kg \cdot s^{-1}}$. Choosing a specific speed $\Omega = 0.422$, the rotational speed is $N = 23562$ rpm. With an efficiency of 84%, the expected output power is 8.7 MW. The geometrical characteristics are listed in Table 1

A numerical test bench Fig. 5 is run before system simulation. The characteristics of the designed turbine that are predicted by the model described in Section 2 for fixed inlet conditions are presented in Fig. 6 where the inlet guide vane angle is varied and in Fig. 7 where the turbine rotation rate is varied.

3.3. System design and off-design simulations

Using a test bench with fixed pressure or flow boundary condition as described in the previous section is an established approach for turbine design. However, the actual usage of the turbine in a closed fluid loop will create different operating conditions in reality. All design parameter changes of the turbine will affect it's boundary

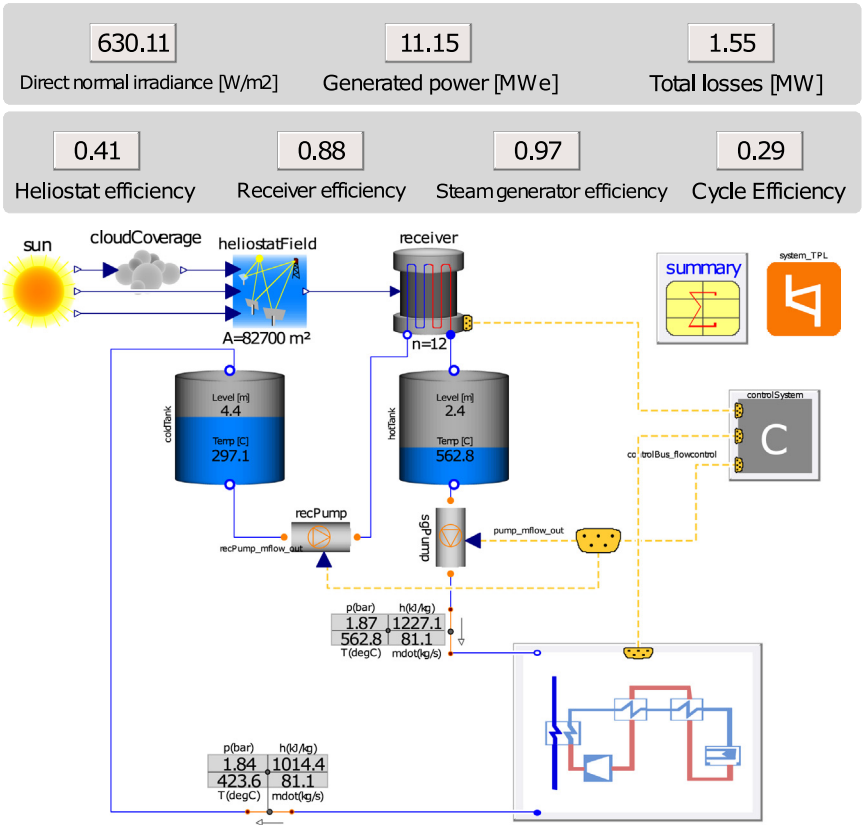

Fig. 3. Solar plant system model including the heliostat field, receiver, hot and cold solar salt storage tanks and fluid loop as well as the Brayton cycle.

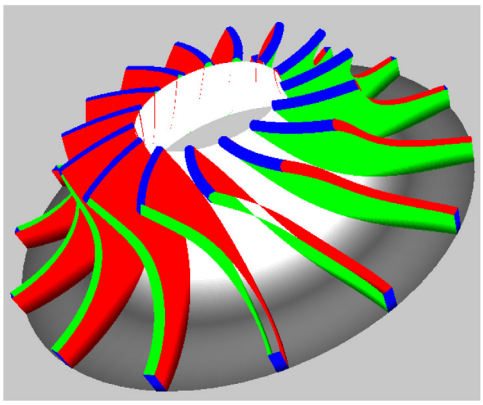

Fig. 4. sCO2 turbine geometry.

conditions due to the thermodynamic coupling in the closed cycle. The optimal design for the turbine integrated into the cycle may therefore look different from those on the test-bench. While for a single design point it is theoretically possible to size components separately on test benches to achieve the optimal design targets, even for the coupled system. In practice, it is not the case. Manufacturing constrains typically lead to compromises in component selection. In addition, the actual operation will include a variety of different operating points. For a

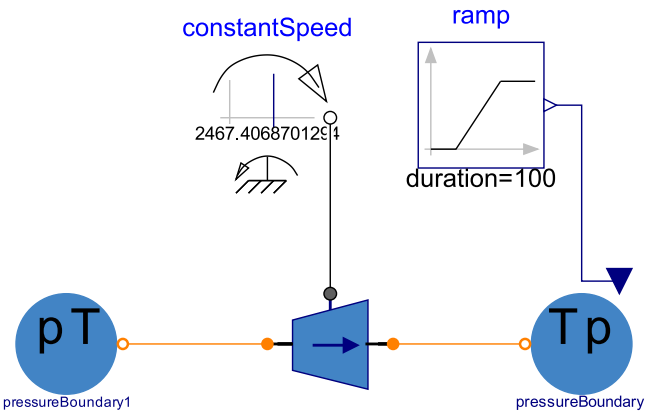

Fig. 5. Simple numerical test bench.

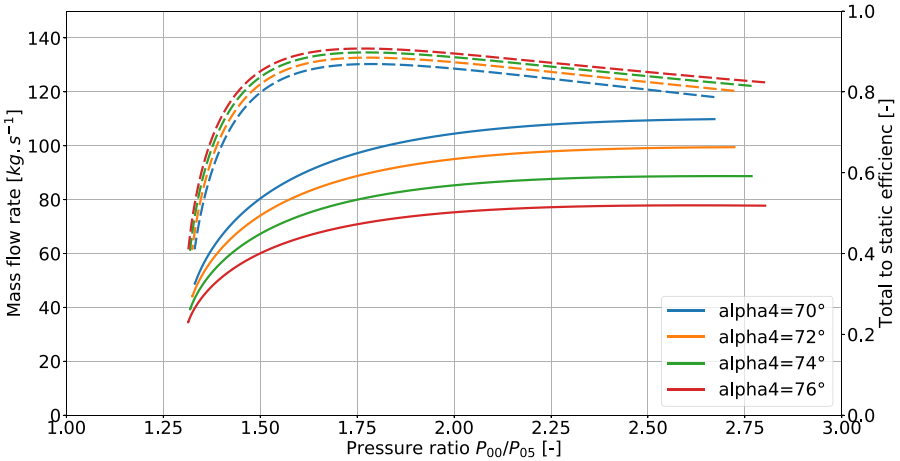

Fig. 6. Turbine performance map for various inlet rotor angle α_4 and $N = 23562$ rpm. Continuous lines: mass flow rate *vs.* pressure ratio, and dashed lines: total to static isentropic efficiency *vs.* pressure ratio.

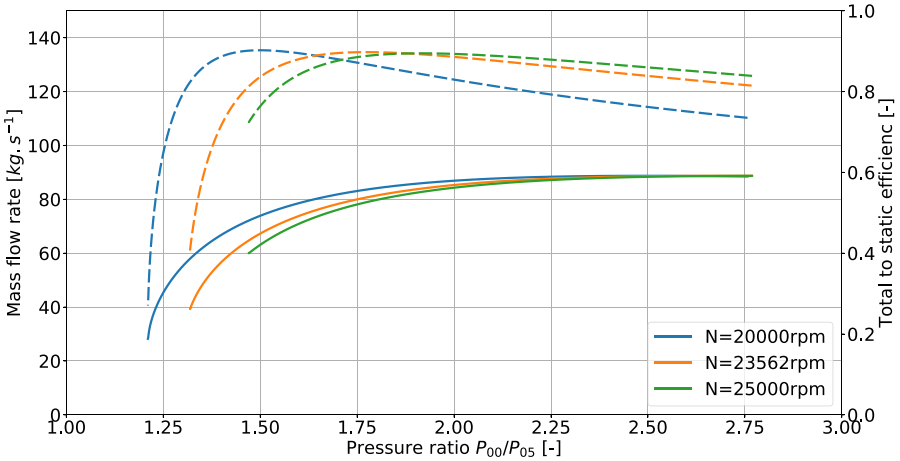

Fig. 7. Turbine performance map for various rotational speed N and $\alpha_4 = 74°$. Continuous lines: mass flow rate *vs.* pressure ratio, and dashed lines: total to static isentropic efficiency *vs.* pressure ratio.

Table 2. Modelica model statistics.

Model type	Nbr of equations	Simulation time in %
Turbine Stodola	31	100
Turbine Meanline	69	130
Solar Plant System	4252	3430

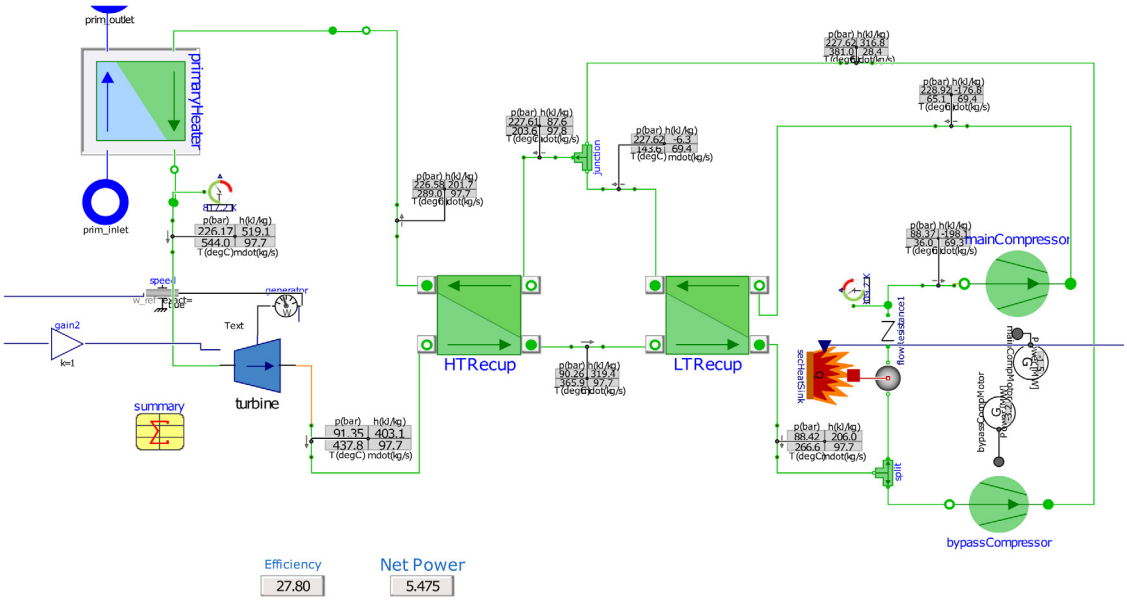

Fig. 8. Supercritical CO2 Bryton cycle model in an offDesign operating point.

super-critical solar power plant, both the consumer side as well as the solar heat source side will introduce variations of load.

Compared to a detailed CFD simulations, the mean-line based turbine model is a computationally lightweight implementation for turbine onDesign and offDesign investigations. The test-bench simulations of the component takes only fractions of a second to solve, even simulating a day of operation of the high-fidelity solar plant introduced in Section 3.1 takes only minutes to solve on conventional office hardware using Modelon Impact solvers. Table 2 gives a comparison on some basic Modelica model metrics, highlighting the fact that the mean-line models complexity is comparable to a simple Stodola based model while the difference is negligible comparing to the resulting plant system model.

In order to improve the design process for solar plants, the presented mean-line turbine model can therefore be integrated into the solar plant system model directly without sacrificing performance. Fig. 8 shows the mean-line turbine model integrated with the sCO2 cycle. The cycle includes the *primaryHeater* in the top-left that takes up heat from the hot solar salt entering the port *prim_inlet*. The heat is transferred to the sCO2 loop (green connection lines). After leaving the *primaryHeater*, the high-pressure, high-temperature CO2 is expanded in the *turbine*. Downstream, the working fluid loop includes a high temperature and low temperature recuperator: *HTRecup* and *LTRecup*, as well as two parallel compression stages *mainCompressor* and *bypassCompressor* with low-pressure heat extraction on the main branch. All components except the mean-line turbine are based on Modelon's VaporCycle Library. The heat exchangers are implemented geometry-based as discretized counterflow, including fluid and metal masses to capture transient effects caused by thermal inertia. The compressor models are conventional map-based components calculating correlations based on supplier maps for flow, pressure-ratio, speed and efficiency.

This setup allows offDesign investigations of different scenarios. As an example, the following scenario is studied:

1. t = 0 min: operation of the cycle at maximum load condition. Hot tank of the solar plant is filled with high temperature molten salt, primary heater of the sCO2 cycle receives 180 kg/s at 630 °C.

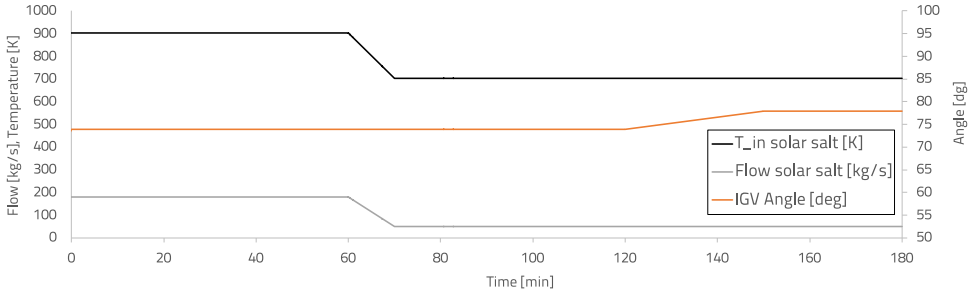

Fig. 9. Cycle inputs for the offDesign investigation.

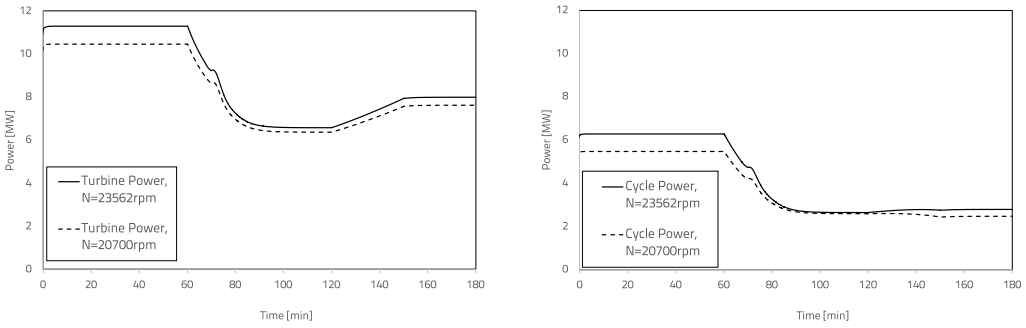

Fig. 10. Outputs of the Solar plant system simulation: turbine power (left) and net cycle power (right).

2. t = 60 min: negative load change. Molten salt flow drops from 180 kg/s to 50 kg/s and temperature to 470 °C.
3. t = 120 min: change of inlet guide-vane position. The inlet guide-vane position and therefore the alpha4 angle inside the turbine is changed from 74° to 78°.

Fig. 9 shows the inputs to the cycle for the example offDesign scenario including a negative load change and an adaption of the IGV position.

In addition to the transient changes, the investigation is combined with a parametric study of the turbine speed, one representing the previously identified reference point at 23562 rpm while a lower speed of 20700 rpm has been added for comparison. For the system design, adding the option to operate at different speed will increase cost, e.g. gear-box or frequency converter need to be added.

Fig. 10 shows the resulting power output for the turbine as well as the full sCO2 cycle for the scenario. The first 60 min, the power output of the turbine is steady at 11.3 MW for the reference speed. While at t = 60 min, when solar salt input power is reduced, the generated power output from the turbine is dropping to 6.5 MW. At t = 120 min, when the IGV angle is increased, the power output increases to 8 MW. Looking at the cycle output power, which is the net difference between the power produced by the turbine and the power consumed by the main compressor and bypass compressor, a power reduction at 60 min can be observed as well. From around 6 MW down to 3 MW. The cycle power increase when increasing the IGV angle is significantly smaller, around 0.2 MW only, indicating a significant increase of the compressor power consumption not explicitly shown here. Looking at the results for the lower turbine speed, the general trends for the turbine output power are the same. However, for the cycle power, changing the IGV angle at 120 min leads to a power reduction instead of an increase.

Fig. 11 shows some internal variables that indicate reasons for these observations. Looking at the turbine inlet pressure, it can be seen that it has a strong correlation with the turbine power. Also it shows that at t = 120 min, when the IGV angle is increased, the changed flow characteristics of the turbine result in an significant increase of the pressure. Thus also explaining the increased power consumption by the compressors indicated earlier.

The turbine efficiency curve shows that for the high power phase until t = 60 min, efficiency for the reference speed is much higher compared to the lower speed which is aligned with the component test bench study. However, for the low load, it shows that reduction of speed can increase the efficiency a lot. Increasing the IGV angle at t =

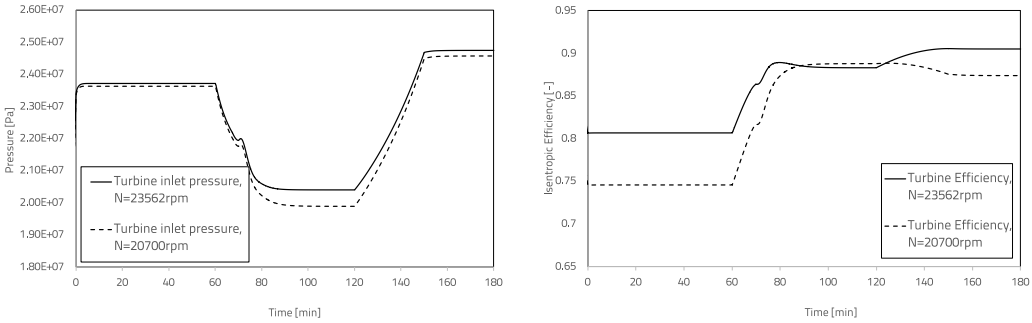

Fig. 11. Outputs of the Solar plant system simulation: turbine inlet pressure (left) and isentropic efficiency (right).

Table 3. SWOT analysis.

Strengths	Weaknesses
• Design and off-design performance prediction • Performance map directly build on geometry • Available information at early stage during system sizing	• Underlying meanline models • Tuning parameters
Opportunities	**Threats**
• Coupled optimization of turbine design with system interactions • System output optimization instead of component efficiency	• Limited accuracy for non-conventional geometries

120 will lead to a decreasing efficiency for the low speed however, while for the reference speed it will improve in this point.

The animated pressure–enthalpy-diagram in the Brayton-Cycle model shown in Fig. 12 gives a more comprehensive picture for analyzing the effects of turbine load and parameter changes in the full cycle in its physical details. Showing the full load (black) compared to the low load states with the default IGV angle (orange) of 74° and the effect of increasing the IGV angle to 78° (blue). Decreasing solar salt temperature results in lower cycle maximum temperatures and enthalpy. Increasing the IGV angle results in a throttling effect that increases the high pressure side as shown previously. The low pressure is controlled by the main and bypass compressors in this scenario. Due to the change in high pressure, both the inlet and outlet temperature state of the turbine will change. The isothermal lines in the diagram around the lower left point of the cycle showing the influence of the critical point which is at 73.8 bar and 31 °C. Towards the critical point, isothermal lines become almost horizontal which implies fluid heat capacities become very large and non-linear and a stable operating point cannot be achieved. Keeping the compressor inlet state well above that region assured stable transient operation while a pure steady-state tool might have identified an operation point at a lower pressure that would not have worked in reality.

Some findings from the example study can be summarized as follows: While little power is available, e.g. due to reduced filling level of the solar salt tank, increasing the IGV angle will lead to better efficiency and better power on reference speed. However, maximum efficiency at low load can be achieved with lower turbine speed, while for maximum power the turbine should be operated at higher speed. Thus demonstrating the optimization potential for different optimization targets: either for maximum efficiency or maximum power output. While often the design target is aiming at best average efficiency, large variations in electricity prices or providing ancillary services to the grid may motivate an operation mode for maximum power instead. Both can be studied in the closed cycle model using the meanline turbine model. A SWOT analysis regarding the integration of turbomachine meanline modeling in system simulation is presented in Table 3

4. Conclusions and perspectives

In this paper, a meanline model for radial inflow turbine operating with real gas has been implemented in MODELICA language for the first time to the authors' best knowledge. This turbine model has been coupled

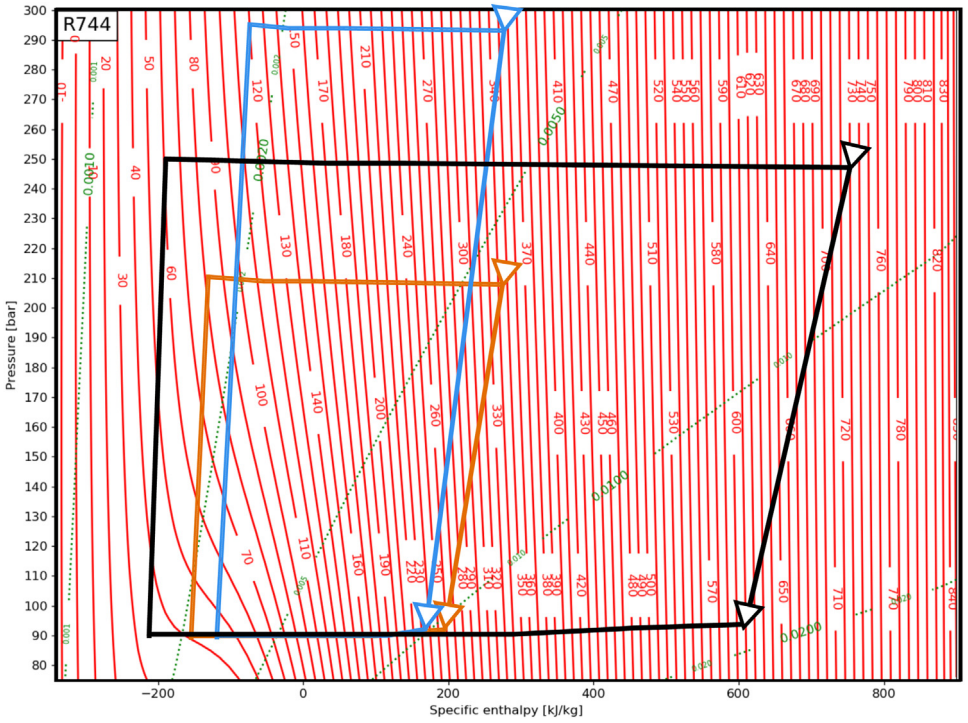

Fig. 12. Comparison of the sCO2 cycle state points in the pH-diagram for a full load point (black), default low load point with IGV = 74° (orange) and optimized low load point with IGV = 78° (blue), turbine expansion highlighted with triangle markers. (For interpretation of the references to color in this figure legend, the reader is referred to the web version of this article.)

with a Brayton super critical CO2 cycle integrated to a concentrated solar power plant with thermal energy storage. The number of equations for the full system model is nearly not affected by the replacement of the Stodola simple turbine model with the proposed meanline approach. The operation of the CSP plant has been simulated for various conditions with the adaptation of the turbine rotational speed and inlet guide vane angle. The results demonstrated the compatibility of the designed turbine with the CSP plant and the variation of turbine efficiency and cycle power for varying and transient conditions. The investigations showed that for the varying load conditions in the solar plant system, an improved operating point has been identified by adjusting the rotational speed and the inlet guide vane angle.

Meanline model included in system simulation will allow the robust and systemic optimization of the turbine coupled with the system for varying conditions. This will improve that performance in the actual working environment. Meanline models provide a first-principle based modeling approach for early stage system design even before expensive turbine map-data from test rigs or CFD simulations is available. While turbine geometry may be used from existing turbines or identified by good engineering assumptions, the presented approach allows studying dynamic system effects especially for new working fluids, e.g. in ORC processes or even multi-component working fluid mixtures. Also for later stages of the system design process, the flexibility of the approach will generate benefit: as shown, variable turbine speed will lead to higher economic outcome during operation which can be evaluated and compared to the additional investment cost.

Declaration of competing interest

The authors declare that they have no known competing financial interests or personal relationships that could have appeared to influence the work reported in this paper.

Data availability

Data will be made available on request.

References

[1] Song J, Wang Y, Wang K, Wang J, Markides CN. Combined supercritical CO2 (SCO2) cycle and organic Rankine cycle (ORC) system for hybrid solar and geothermal power generation: Thermoeconomic assessment of various configurations. Renew Energy 2021;174:1020–35. http://dx.doi.org/10.1016/j.renene.2021.04.124.

[2] White MT, Bianchi G, Chai L, Tassou SA, Sayma AI. Review of supercritical CO2 technologies and systems for power generation. Appl Therm Eng 2021;185(July 2020). http://dx.doi.org/10.1016/j.applthermaleng.2020.116447.

[3] Petrollese M, Cocco D. A multi-scenario approach for a robust design of solar-based ORC systems. Renew Energy 2020;161:1184–94. http://dx.doi.org/10.1016/j.renene.2020.07.120.

[4] Yu H, Helland H, Yu X, Gundersen T, Sin G. Optimal design and operation of an organic Rankine cycle (ORC) system driven by solar energy with sensible thermal energy storage. Energy Convers Manage 2021;244(June):114494. http://dx.doi.org/10.1016/j.enconman.2021.114494.

[5] Binotti M, Astolfi M, Campanari S, Manzolini G, Silva P. Preliminary assessment of sCO2 power cycles for application to CSP solar tower plants. Energy Procedia 2017;105:1116–22. http://dx.doi.org/10.1016/j.egypro.2017.03.475.

[6] Petrollese M, Cocco D. Robust optimization for the preliminary design of solar organic Rankine cycle (ORC) systems. Energy Convers Manage 2019;184(February):338–49. http://dx.doi.org/10.1016/j.enconman.2019.01.060.

[7] Casella F, Leva A. Modelica open library for power plant simulation: Design and experimental validation. In: Proceedings of the 3rd international modelica conference. 2003. p. 41–50.

[8] Quoilin S, Desideri A, Wronski J, Bell I, Lemort V. ThermoCycle: A modelica library for the simulation of thermodynamic systems. In: Proceedings of the 10th international modelica conference, vol. 96, 2014, p. 683–92. http://dx.doi.org/10.3384/ecp14096683.

[9] Wolf V, Bertrand A, Leyer S. Analysis of the thermodynamic performance of transcritical CO2 power cycle configurations for low grade waste heat recovery. Energy Rep 2022;8:4196–208. http://dx.doi.org/10.1016/j.egyr.2022.03.040.

[10] Giovannelli A, Archilei EM, Salvini C. Full-admission radial turbine for waste heat recovery organic Rankine cycles. Energy Rep 2020;6:646–51. http://dx.doi.org/10.1016/j.egyr.2019.09.043.

[11] Yang J, Yang Z, Duan Y. Off-design performance of a supercritical CO2 Brayton cycle integrated with a solar power tower system. Energy 2020;201:117676. http://dx.doi.org/10.1016/j.energy.2020.117676.

[12] Sielemann M, Coïc C, Hübel M, Zhao X, Kyprianidis K. Introduction to multi-point design strategies for aero engines. In: Proceedings of the ASME turbo expo, vol. 6, 2020, http://dx.doi.org/10.1115/GT2020-14912.

[13] Wittenburg R, Hübel M, Holtz D, Müller K. Transient exergy analysis of the dynamic operation of a combined cycle power plant, vol. 2021-July. American Society of Mechanical Engineers, Power Division (Publication) POWER; 2021, http://dx.doi.org/10.1115/POWER2021-64311.

[14] Wittenburg R, Hübel M, Prause H, Gierow C, Reißig M, Hassel E. Effects of rising dynamic requirements on the lifetime consumption of a combined cycle gas turbine power plant. Energy Procedia 2019;158:5717–23. http://dx.doi.org/10.1016/j.egypro.2019.01.562.

[15] Hübel M, Meinke S, Andrén MT, Wedding C, Nocke J, Gierow C, et al. Modelling and simulation of a coal-fired power plant for start-up optimisation. Appl Energy 2017;208(September):319–31. http://dx.doi.org/10.1016/j.apenergy.2017.10.033.

[16] Huebel M, Gierow C, Prause JH, Meinke S, Hassel E. Simulation of ancillary services in thermal power plants in energy systems with high impact of renewable energy, vol. 2. American Society of Mechanical Engineers, Power Division (Publication) POWER; 2017, http://dx.doi.org/10.1115/POWER-ICOPE2017-3258.

[17] Prause JH, Koltermann J, Meinke S, Holtz D, Hassel E. Evaluation of the effects of a load shedding at a lignite power plant. Energy Sci Eng 2021;9(8):1263–73. http://dx.doi.org/10.1002/ese3.890.

[18] Hubel M, Prause JH, Gierow C, Hassel E, Wittenburg R, Holtz D. Evaluation of flexibility optimization for thermal power plants, vol. 2. American Society of Mechanical Engineers, Power Division (Publication) POWER; 2018, http://dx.doi.org/10.1115/POWER2018-7573.

[19] Span R, Wagner W. A new equation of state for carbon dioxide covering the fluid region from the triple-point temperature to 1100 K at pressures up to 800 MPa. 1996, http://dx.doi.org/10.1063/1.555991.

[20] Bell IH, Wronski J, Quoilin S, Lemort V. Pure and pseudo-pure fluid thermophysical property evaluation and the open-source thermophysical property library CoolProp. Ind Eng Chem Res 2014;53(6):2498–508. http://dx.doi.org/10.1021/ie4033999, URL http://pubs.acs.org/doi/abs/10.1021/ie4033999.

[21] Persky R, Sauret E. Loss models for on and off-design performance of radial inflow turbomachinery. Appl Therm Eng 2019;150(October 2018):1066–77. http://dx.doi.org/10.1016/j.applthermaleng.2019.01.042.

[22] Bell I, Quoillin S, Wronski J, Lemort V. Coolprop: An open-source reference-quality thermophysical property library. (1). 2013, ASME ORC 2nd International Seminar on ORC Power Systems - Rotterdam, Netherlands.

[23] Wasserbauer CA, Glassman AJ. FORTRAN program for predicting off-design performance of radial-inflow turbines. Tech. rep. 1975.

[24] Qi J, Reddell T, Qin K, Hooman K, Jahn IH. Supercritical CO2 radial turbine design performance as a function of turbine size parameters. J Turbomach 2017;139(8). http://dx.doi.org/10.1115/1.4035920.

[25] Erbas M, Bıyıko glu A. Design and multi-objective optimization of organic Rankine turbine, international. Int J Hydrog Energy 2015. http://dx.doi.org/10.1016/j.ijhydene.2015.04.143.

[26] Daily JW, Nece RE. Chamber dimension effects on induced flow and frictional resistance of enclosed rotating disks. J Basic Eng 2011. http://dx.doi.org/10.1115/1.3662532.

[27] Baines NC. Radial turbine design. In: Axial and radial turbines. 2003.

[28] G. R. Rodgers C. Performance of a high-efficiency radial/axial turbine. J Turbomach 1987;109(2):151–4.

[29] Edman J, Windahl J. Dynamic modeling of a central receiver CSP system in modelica. In: Proceedings of the 11th international modelica conference, vol. 118, 2015, p. 585–94. http://dx.doi.org/10.3384/ecp15118585.

[30] Ravi AK, Velut S, Srinivasan RV. Modeling of recompression Brayton cycle and CSP plant architectures for estimation of performance and efficiency. In: Proceedings of the 14th international modelica conference. 2021, p. 585–94. http://dx.doi.org/10.3384/ecp21181643.
[31] Aungier RH, Aungier R. Preliminary aerodynamic design of axial-flow turbine stages. In: Turbine aerodynamics: Axial-flow and radial-flow turbine design and analysis. 2010, http://dx.doi.org/10.1115/1.802418.ch6.